

# Online Research @ Cardiff

This is an Open Access document downloaded from ORCA, Cardiff University's institutional repository: <https://orca.cardiff.ac.uk/id/eprint/159210/>

This is the author's version of a work that was submitted to / accepted for publication.

Citation for final published version:

Ye, Jiani, Zhang, Dongsheng, Salli, Sofia, Li, Yajiao, Han, Feiyu, Mai, Yuanqiang, Rosei, Federico, Li, Yongwang, Yang, Yong, Besenbacher, Flemming, Niemantsverdriet, Hans, Richards, Emma ORCID: <https://orcid.org/0000-0001-6691-2377> and Su, Ren 2023. Heterogeneous photocatalytic recycling of FeX<sub>2</sub>/FeX<sub>3</sub> for efficient halogenation of C-H bonds using NaX. *Angewandte Chemie International Edition* 10.1002/anie.202302994 file

Publishers page: <http://dx.doi.org/10.1002/anie.202302994>  
<<http://dx.doi.org/10.1002/anie.202302994>>

Please note:

Changes made as a result of publishing processes such as copy-editing, formatting and page numbers may not be reflected in this version. For the definitive version of this publication, please refer to the published source. You are advised to consult the publisher's version if you wish to cite this paper.

This version is being made available in accordance with publisher policies.

See

<http://orca.cf.ac.uk/policies.html> for usage policies. Copyright and moral rights for publications made available in ORCA are retained by the copyright holders.



# Heterogeneous Photocatalytic Recycling of FeX<sub>2</sub>/FeX<sub>3</sub> for Efficient Halogenation of C H Bonds Using NaX

Jiani Ye<sup>+</sup>, Dongsheng Zhang<sup>+</sup>, Sofia Salli, Yajiao Li, Feiyu Han, Yuanqiang Mai, Federico Rosei, Yongwang Li, Yong Yang, Flemming Besenbacher, Hans Niemantsverdriet, Emma Richards, and Ren Su<sup>\*</sup>

**Abstract:** Environmental-friendly halogenation of C H bonds using abundant, non-toxic halogen salts is in high demand in various chemical industries, yet the efficiency and selectivity of laboratory available protocols are far behind the conventional photolytic halogenation process which uses hazardous halogen sources. Here we report an FeX<sub>2</sub> (X = Br, Cl) coupled semiconductor system for efficient, selective, and continuous photocatalytic halogenation using NaX as halogen source under mild conditions. Herein, FeX<sub>2</sub> catalyzes the reduction of molecular oxygen and the consumption of generated oxygen radicals, thus boosting the generation of halogen radicals and elemental halogen for direct halogenation and indirect halogenation via the formation of FeX<sub>3</sub>. Recycling of FeX<sub>2</sub> and FeX<sub>3</sub> during the photocatalytic process enables the halogenation of a wide range of hydrocarbons in a continuous flow, rendering it a promising method for applications.

## Introduction

The halogenation of C H bonds is an indispensable process for the preparation of precursors for synthetic chemistry, e.g. in the pharmaceutical and polymer industries.<sup>[1]</sup> Photolytic homolysis of elemental halogen (i.e., Cl<sub>2</sub>, Br<sub>2</sub>) under UV irradiation is the most mature halogenation method at industrial scale (Scheme 1A),<sup>[2]</sup> however, such a protocol

relies on the use of molecular halogens, which are toxic, corrosive, and environmentally risky. Additionally, the concentrations of reactants and photogenerated halogen radicals, and the reaction conditions need to be carefully controlled to minimize the formation of over halogenated products and isomers.<sup>[3]</sup> Photolytic halogenation employing organic halogen sources (i.e., N-bromosuccinimide (NBS), N-chlorosuccinimide (NCS)) provides a more controlled synthesis of halogenated chemicals under relative mild reaction conditions (Scheme 1A),<sup>[4]</sup> although the removal of heteroatom centered radicals to avoid the formation of by-products remains a challenge. Additionally, the cost and storage of these unstable halogen reagents need to be considered.<sup>[4b,5]</sup>

The use of non-toxic, inorganic halogen salts, ideally NaBr and NaCl, is the ultimate solution to achieve an eco-friendly halogenation synthesis.<sup>[6]</sup> In the presence of oxidants (i.e., Oxone, Na<sub>2</sub>SO<sub>8</sub>, and H<sub>2</sub>O<sub>2</sub>), halogen radicals are released under irradiation to attack the C(sp<sup>3</sup>) H and C(sp<sup>2</sup>) H bonds (Scheme 1B).<sup>[7]</sup> However, the need of strong oxidants is a disadvantage for the halogenation of molecules with delicate functional groups at a late stage and for sustainable synthesis in general.<sup>[8]</sup> Alternatively, specific transition metal halides (i.e., FeBr<sub>3</sub>, CuCl<sub>2</sub>, NiCl<sub>2</sub>) can be excited to release halogen radicals under mild conditions, which appears attractive for C H bond halogenation.<sup>[5a,9]</sup> Note that halogen radicals form together with oxygen radicals,<sup>[10]</sup> resulting in the formation of oxidation by-products during the process, eventually leading to poor selectivities. Maldotti et al. show that FeCl<sub>3</sub> embedded in an

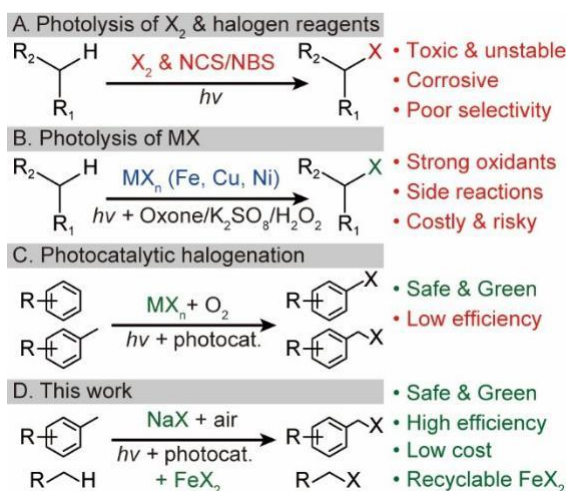
[\*] J. Ye,<sup>+</sup> D. Zhang,<sup>+</sup> Y. Li, F. Han, Y. Mai, Prof. Dr. F. Rosei, Prof. Dr. R. Su  
Soochow Institute for Energy and Materials InnovationS (SIEMIS), Soochow University  
Suzhou, 215006 (China) E-mail: suren@suda.edu.cn

J. Ye,<sup>+</sup> D. Zhang,<sup>+</sup> Prof. Dr. Y. Li, Prof. Dr. Y. Yang,  
Prof. Dr. H. Niemantsverdriet, Prof. Dr. R. Su  
SynCat@Beijing Synfuels China Technology Co. Ltd.  
Leyuan South Street II, No.1, Yanqi Economic Development Zone C#, Huairou District, Beijing, 101407 (China)  
SynCat@Beijing

S. Salli, Dr. E. Richards  
School of Chemistry, Cardiff University  
Park Place, Cardiff, CF10 3AT (UK)

Prof. Dr. F. Rosei  
Center for Energy, Materials and Telecommunications,  
Institut National de la Recherche Scientifique  
1650 Boulevard Lionel-Boulet, Varennes, J3X 1P7 Québec  
(Canada) Prof. Dr. Y. Li, Prof. Dr. Y. Yang  
State Key Laboratory of Coal Conversion, Institute of Coal Chemistry  
Taiyuan, 030001 (China)  
Prof. Dr. F. Besenbacher  
Interdisciplinary Nanoscience Center, Aarhus University  
Gustav Wieds Vej 14, 8000 Aarhus (Denmark)  
Prof. Dr. H. Niemantsverdriet  
SynCat@DIFFER Syngaschem BV  
6336 HH Eindhoven (The Netherlands)

[\*] These authors contributed equally to this work.



**Scheme 1.** Solutions for photolytic and photocatalytic halogenation of hydrocarbons along with pros and cons in green and red, respectively.

anion exchange resin enables the chlorination of cycloalkanes with decent selectivity under irradiation.<sup>[11]</sup> Although this system could be recycled for three times by dosing ClO<sub>2</sub>, the long-term continuous synthesis remained a challenge. Therefore, a catalytic system that enables halogenation of C-H bonds with high selectivity, ideally using non-toxic inorganic salts as the halogen source under oxidants free and ambient conditions would be of great practical importance.

Heterogeneous photocatalysis employing tailored semiconductor materials can generate desired radical species under mild conditions,<sup>[12]</sup> thus providing an eco-friendly platform for halogenation reactions. A few works show that elemental Br and Cl at a level of 0.3 mM can be generated via photo-oxidation of Br<sup>-</sup> and Cl<sup>-</sup> anions using TiO<sub>2</sub> based photocatalysts under acidic conditions.<sup>[13]</sup> Markushyna et al. report the successful synthesis of sulfonyl chlorides and aromatic halides using a polymeric heptazine imide photocatalyst (Scheme 1C).<sup>[14]</sup> Similarly, a Cu@CuCl photocatalyst has been reported for the synthesis of benzyl chloride using bittern (a salt precipitate from sea water) as the halogen source.<sup>[15]</sup> While the halogen anions are oxidized by the photogenerated holes to produce molecular chlorine, the photogenerated electrons need to be scavenged by molecular oxygen spontaneously. Therefore, the slow oxygen reduction reaction severely limits the generation rate of active halogen species, resulting in an inefficient halogenation under ambient conditions. This calls for a photo-catalytic system enabling fast oxygen reduction to promote the formation of halogen radicals from oxidation of abundant metal halides.

Herein, we report an FeX<sub>2</sub>-semiconductor system for the photocatalytic halogenation of C-H bonds using NaX as halogen source in the presence of acid under ambient conditions (X = Br, Cl). The Fe<sup>2+</sup> cation promotes the in situ photogeneration of halogen radicals from NaX by accelerating the oxygen reduction reaction, resulting in the formation of FeX<sub>3</sub>, which halogenates the reactants under irradiation,

after which Fe<sup>3+</sup> reduces back to the Fe<sup>2+</sup> cation. The catalytic redox cycle of Fe<sup>2+</sup>/Fe<sup>3+</sup> allows the use of abundant NaBr and NaCl as the halogen source and affords a high quantum efficiency (QE) under atmospheric environment. The potential of the FeX<sub>2</sub>-semiconductor system in terms of stability, substrate scope and photocatalytic synthesis in flow mode are discussed as well.

## Results and Discussion

The photo-induced bromination of toluene is chosen as a model reaction and is performed under different conditions (Figure 1 and Figure S1). When solely anhydrous FeBr<sub>3</sub> powders (0.3 mmol) are added in toluene, photolytic bromination of toluene into benzyl bromide occurs with pseudo first-order reaction kinetics ( $k = 0.033 \text{ min}^{-1}$ ) under 365 nm irradiation at ambient conditions (Figure 1a). This process is initiated by the photo-excitation of FeBr<sub>3</sub> and formation of Br radicals, as reported previously.<sup>[16]</sup> The formation of benzyl bromide (0.3 mmol) is accompanied by the complete reduction of FeBr<sub>3</sub> into FeBr<sub>2</sub> (Figure S1), which cannot be used for the bromination in the consecutive cycle (Figure 1b). When TiO<sub>2</sub>, FeBr<sub>2</sub> (0.3 mmol) and NaBr (0.3 mmol) are added into toluene under irradiation, benzyl bromide evolves with a rate constant of  $0.026 \text{ min}^{-1}$ , which is only slightly slower than the photolytic process using solely FeBr<sub>3</sub> (Figure 1c). Note that formation and consumption of Fe<sup>3+</sup> is observed during this process (Figure S2), indicating that the Fe<sup>2+</sup>/Fe<sup>3+</sup> redox reactions are involved in the bromination. A total amount of 0.3 mmol benzyl bromide and the disappearance of Fe<sup>3+</sup> species suggest that all Br originate from NaBr. This is further confirmed by dosing an additional 0.3 mmol NaBr into the reaction system under irradiation, upon which the same amount of benzyl bromide forms with identical reaction kinetics (Figure 1d). Identical evolution of Fe<sup>3+</sup> is also observed in the second cycle, indicating that TiO<sub>2</sub> catalyzes the generation of FeBr<sub>3</sub> under irradiation, which then brominates toluene via photolysis. Concentrated H<sub>2</sub>SO<sub>4</sub> (30  $\mu\text{L}$ , 18.2 M) is pre-added into the toluene solution to facilitate the formation of reactive halogen species via reducing the adsorption of OH<sup>-</sup> anions thus avoiding the formation of unwanted reactive oxygen species (ROS).<sup>[17]</sup> Additionally, dissociated H<sub>2</sub>SO<sub>4</sub> leads to saturation of SO<sub>4</sub><sup>2-</sup> anions in the solvent, and is beneficial to shift the reaction equilibrium of photocatalytic generation of active halogen species forward. In comparison, when TiO<sub>2</sub> and NaBr are added to toluene in the absence of FeBr<sub>2</sub>, only trace amounts of benzaldehyde and benzyl alcohol are produced under irradiation (Table S1). In addition, the formation of reactive halogen species is exclusively via the photocatalytic process, as no bromination of toluene takes place in the absence of a photocatalyst but in the presence of sulfuric acid (Table S1).

A distinct color change of the suspension is observed during photocatalytic bromination of toluene in the presence of TiO<sub>2</sub>, FeBr<sub>2</sub>, and NaBr, as demonstrated by the centrifuged reaction solution after different irradiation times (Figure 1e). Prior to irradiation, the toluene solution

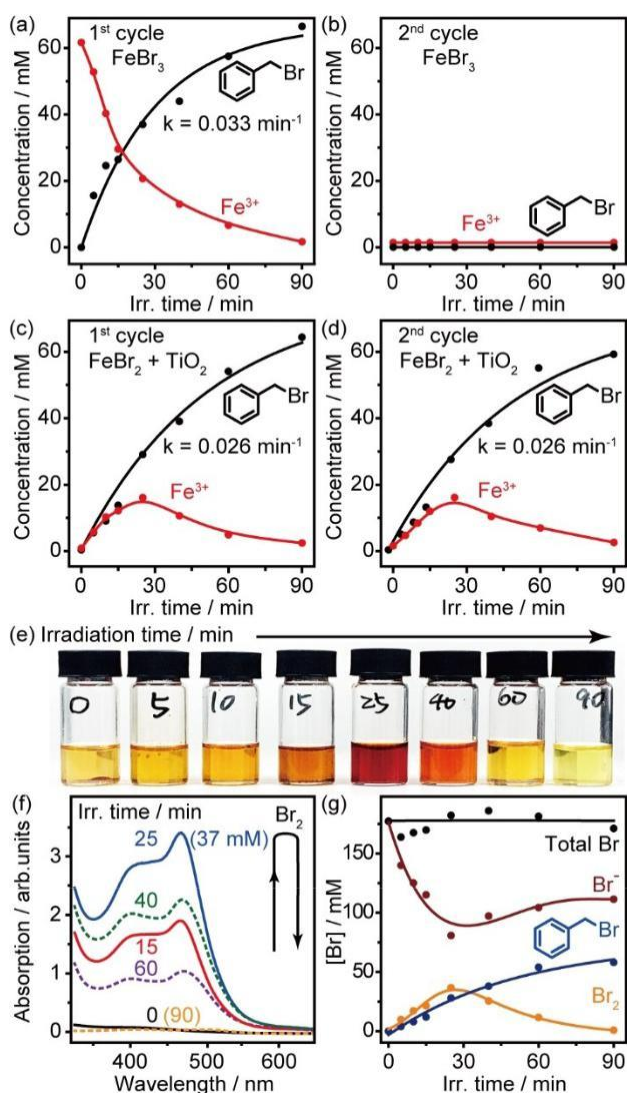


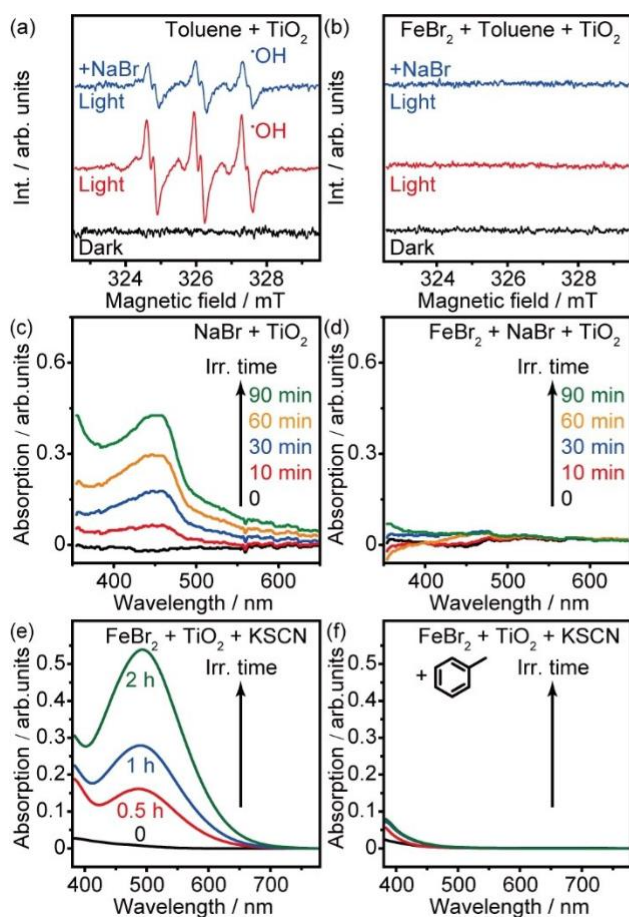
**Figure 1.** Photocatalytic bromination of toluene. a) and b) Conventional photolytic bromination of toluene by  $\text{FeBr}_3$  for two consecutive runs; Reaction conditions: 0.3 mmol  $\text{FeBr}_3$  and 20  $\mu\text{L}$  concentrated  $\text{H}_2\text{SO}_4$  (18.2 M) in 5 mL toluene under 1 bar air at RT, irradiated under 365 nm LED ( $75 \text{ mWcm}^{-2}$ ). c) and d)  $\text{FeBr}_2$ - $\text{TiO}_2$  enabled continuous photocatalytic bromination of toluene using NaBr as the bromine source. Reaction conditions: 0.3 mmol  $\text{FeBr}_2$ , 10 mg  $\text{TiO}_2$ , 0.3 mmol NaBr and 30  $\mu\text{L}$  concentrated  $\text{H}_2\text{SO}_4$  in 5 mL toluene under 1 bar air at RT, irradiated under 365 nm LED ( $75 \text{ mWcm}^{-2}$ ). e) and f) image and UV/Vis spectra of photocatalytic toluene bromination using  $\text{FeBr}_2$ - $\text{TiO}_2$  with NaBr. The solution was diluted 3 times for UV/Vis spectroscopy. g) Evolution of Br species and mass balance during photocatalytic bromination of toluene.

displays a light-yellow color due to the slightly soluble of  $\text{FeBr}_2$  (Figure S3). The solution gradually turns dark red upon increasing the irradiation time to 25 min, and fades back to light-yellow after prolonged irradiation. UV/Vis spectroscopy of the centrifuged solution suggests that the color change is caused by the evolution of elemental Br, as evidenced by the characteristic absorption peak at 470 nm (Figure 1f). The concentration of  $\text{Br}_2$  reaches a maximum of 37 mM at 25 min, which is 1–2 orders of magnitude higher as

compared to other photocatalytic systems in the absence of  $\text{Fe}^{2+}/\text{Fe}^{3+}$  species.<sup>[13–15]</sup> Note that the photogenerated  $\text{Br}_2$  is completely consumed over the course of the reaction, revealing an eco-friendly process. Additionally, the evolution of Br anions during photocatalytic bromination of toluene has been quantitatively analyzed by ion chromatography (IC) and plotted together with  $\text{Br}_2$  and benzyl bromide (Figure 1g and Figure S4). The reaction consists of a series of consecutive reactions with  $\text{Br}_2$  as the intermediate.<sup>[18]</sup> A sharp decrease of Br is accompanied by the formation of  $\text{Br}_2$  and benzyl bromide in the early stage of the reaction ( $t < 25$  min). Benzyl bromide forms continuously by consuming the photogenerated  $\text{Br}_2$ , resulting in a complete depletion of  $\text{Br}_2$  and an equal increase of Br-anions ( $t > 25$  min). The mass balance of Br species is well preserved over the course of the reaction.

The ferrous salt promotes the photocatalytic oxidation of Br anions by accelerating the oxygen reduction half reactions, as evidenced by the evolution of oxygen radicals and  $\text{H}_2\text{O}_2$ . Electron spin resonance (ESR) spectroscopy using phenylbutylnitron (PBN) as the spin trap shows that a significant amount of hydroxyl radical ( $\text{OH}^\cdot$ ) is observed upon irradiation of a  $\text{TiO}_2$ -toluene suspension in the absence of  $\text{Fe}^{2+}$  (red curve, Figure 2a).<sup>[19]</sup> The addition of NaBr (0.3 mmol) reduces the concentration of generated  $\text{OH}^\cdot$  but without producing a detectable quantity of Br radicals (blue curve, Figure 2a).<sup>[20]</sup> The assignment of the hydroxyl radical is further confirmed by additional systematic ESR analysis (Figure S5) and a reference.<sup>[21]</sup> In contrast, the signal of  $\text{OH}^\cdot$  radicals vanishes completely when  $\text{FeBr}_2$  is added into an irradiated  $\text{TiO}_2$ -toluene suspension, regardless of the presence of NaBr (red and blue curves, Figure 2b). The evolution of  $\text{H}_2\text{O}_2$  is probed by UV/Vis spectrometry using a  $\text{CuSO}_4$  :2,9-dimethyl-1,10-phenanthroline (DMP) titrant (Figure S6).<sup>[22]</sup> A gradual increase of the absorption peak at 454 nm is observed in the absence of  $\text{FeBr}_2$ , indicating accumulation of photogenerated  $\text{H}_2\text{O}_2$  ( $\blacklozenge$  0.3 mM at 90 min, Figure 2c). Notably, the addition of  $\text{FeBr}_2$  results in no detectable absorption attributed to  $\text{H}_2\text{O}_2$  throughout the entire irradiation course (Figure 2d). Since  $\text{Fe}^{2+}$  catalyzes the dissociation of  $\text{H}_2\text{O}_2$  and subsequently oxidizes into  $\text{Fe}^{3+}$  via the well-known Fenton reaction,<sup>[23]</sup> it indicates that the  $\text{Fe}^{2+}/\text{Fe}^{3+}$  redox couple is recycled under irradiation, resulting in a rapid, continuous dissipation of both  $\text{OH}^\cdot$  radicals and  $\text{H}_2\text{O}_2$ . Thus, the photogenerated ROS are rapidly consumed in the oxidation of  $\text{Fe}^{2+}$  and can therefore not be captured by the spin trap. Such fast removal of ROS is crucial for the selective halogenation of hydrocarbons, as these would otherwise lead to the production of unwanted oxidized byproducts (e.g., carbonyls, alcohols).<sup>[10]</sup>

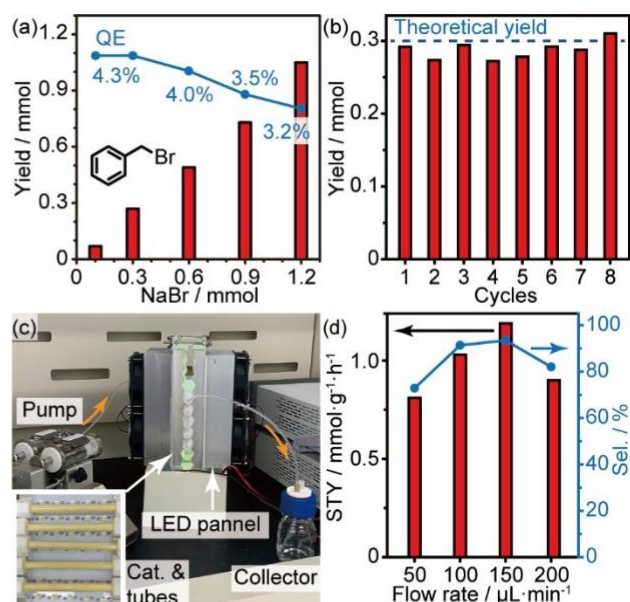
We have further studied the effect of  $\text{Fe}^{2+}$  in accelerating the photo-generation and donation of Br radicals by UV/Vis spectroscopy using KSCN as the titrant (Figures 2e and f). Upon irradiation, the accumulation of Br radical is observed in an  $\text{FeBr}_2$ - $\text{TiO}_2$ -isopropanol suspension using NaBr as the bromine source, as evidenced by the absorption peak at 495 nm. As expected, no Br radical is produced in the absence of  $\text{FeBr}_2$  under otherwise identical reaction conditions (Figure S7a). Remarkably, the formation of Br



**Figure 2.** Promotion mechanisms. a) and b) ESR spectra of the  $\text{TiO}_2$ -toluene suspension without and with  $\text{FeBr}_2$  (30  $\mu\text{mol}$ ). Reaction conditions: 10 mg  $\text{TiO}_2$  in 200  $\mu\text{L}$  toluene with 80 mM PBN, irradiated by a Xe lamp at RT for 1.5 min. c) and d) UV/Vis spectra probing the  $\text{H}_2\text{O}_2$  evolution of a  $\text{TiO}_2$ -NaBr-toluene suspension without and with  $\text{FeBr}_2$  (0.3 mmol). Reaction conditions: 0.3 mmol NaBr, 10 mg  $\text{TiO}_2$  and 30  $\mu\text{L}$  concentrated  $\text{H}_2\text{SO}_4$  in 5 mL toluene under 1 bar air at RT, irradiated under 365 nm LED (75  $\text{mWcm}^{-2}$ ). e) and f) UV/Vis spectra probing the Br radical evolution of a  $\text{TiO}_2$ - $\text{FeBr}_2$ -isopropanol suspension without and with toluene. Reaction conditions: 0.3 mmol  $\text{FeBr}_2$ , 10 mg  $\text{TiO}_2$ , 0.3 mmol NaBr and 30  $\mu\text{L}$  concentrated  $\text{H}_2\text{SO}_4$  in 5 mL KSCN-isopropanol or KSCN-toluene solution under 1 bar air at RT, irradiated under 365 nm LED (75  $\text{mWcm}^{-2}$ ).

radical is completely quenched by replacing isopropanol with toluene as the solvent (Figure 2f). This suggests that the photogenerated Br radicals are rapidly consumed by toluene, as confirmed by the formation of benzyl bromide according to gas chromatograph mass spectrometry analysis (GC-MS, Figure S7b). Similar phenomena are observed when  $\text{FeBr}_3$  is subjected to irradiation in isopropanol and toluene (Figures S7c and S7d), indicating that the introduction of  $\text{TiO}_2$  does not affect the generation and donation of bromine radicals.

The  $\text{FeBr}_2$ - $\text{TiO}_2$  system performs favorably for the photocatalytic bromination of toluene under more practical reaction conditions as well. Upon increasing the quantity of NaBr in the reaction suspension, a proportional increase in benzyl bromide production is observed (Figure 3a). A high

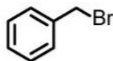
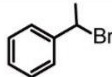
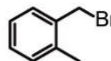
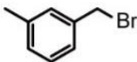
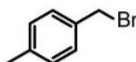
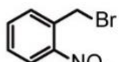
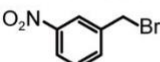
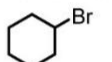
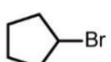
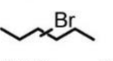
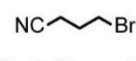
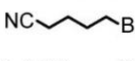
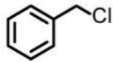
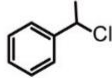
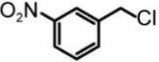
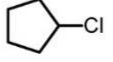
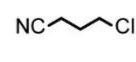
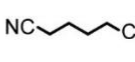


**Figure 3.** Performance and productivity. a) The effect of NaBr loading on the synthesis of benzyl bromide by photocatalytic bromination of toluene. b) Stability of the  $\text{FeBr}_2$ - $\text{TiO}_2$  system for continuous photocatalytic bromination of toluene. Reaction conditions: 0.3 mmol  $\text{FeBr}_2$ , 10 mg  $\text{TiO}_2$ , 0.3 mmol NaBr and 30  $\mu\text{L}$  concentrated  $\text{H}_2\text{SO}_4$  in 5 mL toluene under 1 bar air at RT, irradiated under 365 nm LED (75  $\text{mWcm}^{-2}$ ). c) and d) Apparatus image and the performance of continuous photocatalytic flow synthesis of benzyl bromide using the  $\text{TiO}_2$ - $\text{FeBr}_2$  system. Reaction conditions: 2.1 mmol  $\text{FeBr}_2$ , 70 mg  $\text{TiO}_2$ , 4.5 mmol NaBr, 7 g silica gel and 300  $\mu\text{L}$  concentrated  $\text{H}_2\text{SO}_4$  in 50 mL toluene- $\text{CH}_3\text{CN}$  solution under 1 bar air at RT, irradiated under 365 nm LED (36  $\text{mWcm}^{-2}$ ).

QE of  $\blacklozenge$  4.3% is achieved in the presence of up to 0.3 mmol of NaBr (Note S1). A slight decrease of QE at higher loadings of NaBr is attributed to the aggravated scattering of incident light caused by the insoluble NaBr crystallites. The  $\text{FeBr}_2$ - $\text{TiO}_2$  system can be recycled 8 times consecutively by simply adding a further 0.3 mmol of NaBr during each cycle (Figure 3b). The yield of benzyl bromide in each cycle is close to the theoretical yield at a constant irradiation time of 90 min, indicating a high stability of the system for wide-scale applications. We have further assembled a flow system with 520 mg  $\text{FeBr}_2$ - $\text{TiO}_2$  mixtures (6.5:1 in mass ratio) packed into quartz tubes for the continuous photo-catalytic synthesis of benzyl bromide (Figures 3c, S8–S9, and Note S2). A satisfactory space-time yield (STY, 1.2  $\text{mmol g}^{-1} \text{h}^{-1}$ ) and a high selectivity (> 93%) to benzyl bromide are achieved at a considerably high flow rate (150  $\mu\text{Lmin}^{-1}$ ). The flow system with optimized light absorption renders its potential for scale-up (Figure 3d). In this sense, NaBr and NaCl are the cheapest halogen sources possible (0.17 and 0.02  $\text{Emol}^{-1}$ , respectively), which is attractive for production at scale (Table S2).

The  $\text{FeX}_2$ - $\text{TiO}_2$  system shows satisfactory performance in the photocatalytic halogenation of a series of hydrocarbons in either flow or batch systems under mild reaction conditions (Table 1, Figures S10–27). External standard method is used for quantitative analysis of products (Fig-

**Table 1:** Substrate scope. Halogenation of hydrocarbons catalyzed by the TiO<sub>2</sub>-FeX<sub>2</sub> system with NaBr or NaCl as halogen sources.

$\text{R}_1\text{-CH}_2\text{-R}_2\text{(H)} \xrightarrow[\text{air}]{\text{photocatalyst FeX}_2, \text{NaX}, h\nu, \text{RT}}$ $\text{R}_1\text{-CH(Br)-R}_2\text{(H)} \text{ 2} \quad \text{or} \quad \text{R}_1\text{-CH(Cl)-R}_2\text{(H)} \text{ 3}$		
 <b>2a</b> , 1.45 mmol <sup>a</sup> sel. 94%	 <b>2b</b> , 1.21 mmol <sup>a</sup> sel. 93%	 <b>2c</b> , 0.93 mmol <sup>a</sup> sel. 86%
 <b>2d</b> , 0.98 mmol <sup>a</sup> sel. 89%	 <b>2e</b> , 1.29 mmol <sup>a</sup> sel. 87%	 <b>2f</b> , 0.96 mmol <sup>a</sup> sel. 87%
 <b>2g</b> , 0.84 mmol <sup>a</sup> sel. 86%	 <b>2h</b> , 1.05 mmol <sup>b</sup> sel. 87%	 <b>2i</b> , 0.78 mmol <sup>b</sup> sel. 70%
 <b>2j</b> , 0.85 mmol <sup>b</sup> sel. 55%	 <b>2k</b> , 1.55 mmol <sup>b</sup> sel. 63%	 <b>2l</b> , 1.76 mmol <sup>b</sup> sel. 32%
 <b>3a</b> , 1.21 mmol <sup>c</sup> sel. 87%	 <b>3b</b> , 0.83 mmol <sup>c</sup> sel. 85%	 <b>3c</b> , 0.82 mmol <sup>c</sup> sel. 87%
 <b>3d</b> , 0.75 mmol <sup>d</sup> sel. 80%	 <b>3e</b> , 2.88 mmol <sup>e</sup> sel. 55%	 <b>3f</b> , 2.88 mmol <sup>e</sup> sel. 46%

Reaction conditions: [a] 2.1 mmol FeBr<sub>2</sub>, 70 mg TiO<sub>2</sub>, 4.5 mmol NaBr and 300  $\mu\text{L}$  concentrated H<sub>2</sub>SO<sub>4</sub> in 60 mL substrate-CH<sub>3</sub>CN solution under 365 nm irradiation (36 mWcm<sup>-2</sup>) for 7 h in a flow reactor (150  $\mu\text{Lmin}^{-1}$ ). [b] 0.3 mmol FeBr<sub>2</sub>, 10 mg TiO<sub>2</sub>, 2.0 mmol NaBr and 30  $\mu\text{L}$  concentrated H<sub>2</sub>SO<sub>4</sub> in 25 mL substrate solution under 365 nm irradiation for 24 h (75 mWcm<sup>-2</sup>) in a 50 mL round bottom flask.

[c] 2.1 mmol FeCl<sub>2</sub>, 70 mg g-C<sub>3</sub>N<sub>4</sub>, 4.5 mmol NaCl and 300  $\mu\text{L}$  concentrated HCl (12.1 M) in 40 mL substrate-CH<sub>3</sub>CN solution under 410 nm irradiation for 3.5 h (55 mWcm<sup>-2</sup>) in a flow reactor (200  $\mu\text{Lmin}^{-1}$ ).

[d] 0.3 mmol FeCl<sub>2</sub>, 10 mg g-C<sub>3</sub>N<sub>4</sub>, 2.0 mmol NaCl and 30  $\mu\text{L}$  concentrated HCl in 25 mL substrate solution under 410 nm irradiation for 24 h (75 mWcm<sup>-2</sup>) in a 50 mL round bottom flask. [e] 0.3 mmol FeCl<sub>2</sub>, 10 mg g-C<sub>3</sub>N<sub>4</sub>, 3.0 mmol NaCl and 30  $\mu\text{L}$  concentrated HCl in 5 mL substrate solution for 2 h in a 10 mL round bottom flask. All reactions are performed under 1 bar air at RT. Quantity and selectivity are determined by GC and GC-MS.

ure S28). The bromination of toluene and ethylbenzene shows a high selectivity to the corresponding bromides (**2a** and **2b**) with high quantities (> 1.2 mmol) within an irradiation course of 7 h in the flow system. An additional methyl groups as an electron donating group (EDG) on *o*-, *m*-, and *p*- sites of toluene exert negligible effects on the bromination (**2c–2e**). Interestingly, the presence of -NO<sub>2</sub> as a strong electron withdrawing group (EWG) also does not affect the bromination towards the target products negatively (**2f** and **2g**). Bromination of cyclohexane and cyclopentane (**2h** and **2i**) can be also achieved in a batch reactor

with decent selectivity but a low bromination rate compared with that of toluene and its derivatives, due to the high bond dissociation energy (BDE) of cycloalkanes. The bromination of *n*-hexane results in two single brominated substituents at positions 2° and 3° (**2j**) with a total selectivity of 55% and a molar ratio of 1:1. Aliphatic nitriles can be converted into corresponding bromides in a batch reactor with prolonged irradiation (24 h), though the selectivity and productivity need to be further improved (**2k** and **2l**). The distribution of byproducts for all substrates is shown in Table S3.

Efficient photocatalytic chlorination is achieved by employing graphitic carbon nitride (g-C<sub>3</sub>N<sub>4</sub>) in combination with FeCl<sub>2</sub>, using NaCl as chlorine source under visible light irradiation (410 nm). The selective conversion of toluene, ethylbenzene, and *m*-nitrotoluene to the corresponding chlorides (**3a** and **3c**) is realized at mmol scale in 3.5 h. Synthesis of chlorocyclopentane (**3d**) is highly selective but proceeds only slowly in a batch reactor (24 h for 0.75 mmol). In comparison, relatively high quantities of nitrile chlorides are produced (**3e** and **3f**), but at moderate selectivities, as obtained in the batch reactor for photocatalytic conversion of aliphatic nitriles (2 h). Note that bibenzyl is the main product when pristine TiO<sub>2</sub> is employed as the photocatalyst (Figure S29), formed via the rapid hydrodehalogenation of photogenerated benzyl chloride.<sup>[24]</sup> In comparison, pristine g-C<sub>3</sub>N<sub>4</sub> presents a very slow reaction rate for the hydro-dehalogenation process, thus resulting in a high selectivity to benzyl chloride.<sup>[25]</sup>

Additionally, the chlorination of a series of hydrocarbons with high conversion and selectivity by using a FeCl<sub>2</sub>-Pd/TiO<sub>2</sub> photocatalytic system in acetonitrile solution (Figure 4). Here metallic Pd nanoparticles are supported on TiO<sub>2</sub>, serving as a cocatalyst to facilitate the hydrogen abstraction from the methyl group of toluene (Table S4). A considerable (80%) conversion of toluene (20 mM) is achieved in 8 h of 365 nm irradiation with a high selectivity (♦ 90%) to benzyl chloride (Figure 4a). The major byproduct is bibenzyl (♦ 10%), which is produced via the dehalogenative coupling of the photogenerated benzyl chloride (Figure S30). A much smaller rate constant (0.22 h<sup>-1</sup>) compared to that of using toluene as a solvent (0.026 min<sup>-1</sup>) is caused by a concentration effect (20 mM vs. 9.4 M). Selective synthesis of benzyl chloride is viable even at higher toluene concentrations (Figure 4b). A satisfactory conversion (> 70%) can be realized up to 100 mM of toluene within an irradiation time of 8 h. Noticeably, a reasonable QE of 1.1% is achieved for the conversion of 100 mM toluene due to the relatively high concentration. Both the conversion and selectivity dropped significantly when the concentration of toluene is increased to 200 mM. Furthermore, selective synthesis of a series of chlorinated hydrocarbons listed in Table 1 can be realized with high conversion of the corresponding precursors (Figure 4c), confirming the potential for applications in comparison with reported light-induced protocols (Table S5).

We propose the mechanism of photocatalytic halogenation of hydrocarbons promoted by FeX<sub>2</sub> (Scheme 2). Upon irradiation, the halogen anions and molecular oxygen are oxidized and reduced by the photogenerated holes and

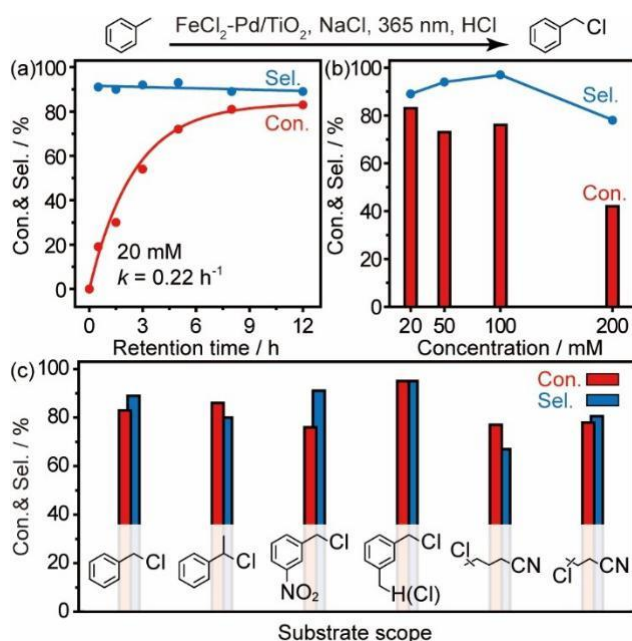
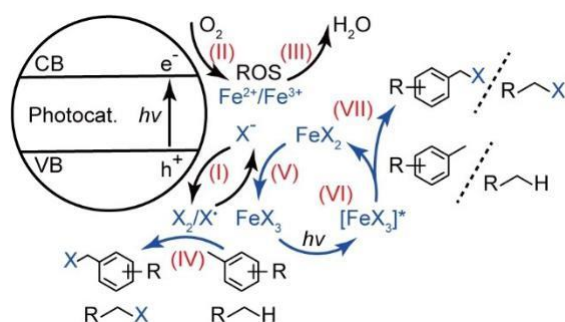


**Figure 4.** Complete photocatalytic chlorination. a) and b) Time profiling and concentration effect for the chlorination of toluene (20–200 mM). c) complete chlorination of a series of hydrocarbons (20 mM). Reaction conditions: 0.3 mmol  $\text{FeCl}_2$ , 10 mg  $\text{Pd/TiO}_2$  (1 wt%), 0.6 mmol  $\text{NaCl}$  (2 mmol for the conversion 200 mM toluene) and 30  $\mu\text{L}$  concentrated  $\text{HCl}$  (12.1 M) in 5 mL  $\text{MeCN}$  at RT, irradiated under 365 nm LED (75  $\text{mWcm}^{-2}$ ). Irradiation time is 8 h for concentration effect and substrate scope.



**Scheme 2.** Proposed Scheme for the photocatalytic recycling of  $\text{FeX}_2/\text{FeX}_3$  for efficient and selective halogenation of C-H bonds.

electrons, producing halogen radicals and ROS ( $\cdot\text{OH}$ ,  $\text{H}_2\text{O}_2$ ), respectively (Steps I and II). The  $\text{Fe}^{2+}$  cations catalyze the generation and dissociation of ROS and are oxidized into  $\text{Fe}^{3+}$  cations, resulting in the rapid consumption of molecular oxygen (Steps II and III). The fast removal of ROS reduces the risk of forming unwanted carbonyls and alcohols, which is beneficial for selective halogenation. Meanwhile, the accelerated  $\text{O}_2$  reduction reaction leads to a rapid generation of halogen radical and elemental halogen, which either directly halogenate the hydrocarbons (Step IV) or oxidize the  $\text{FeX}_2$  to  $\text{FeX}_3$  for photolytic halogenation under irradiation (Steps V and VI). The  $\text{FeX}_3$  is reduced back to  $\text{FeX}_2$  after donating X to the hydrocarbons (Step VII), which participates in oxygen reduction and X radical

consumption to complete the catalytic cycle. The process enables the use of  $\text{NaBr}$  and  $\text{NaCl}$  as the halogen sources, leading to an efficient recycling of ferrous/ferric salts for the continuous photocatalytic halogenation under mild conditions.

## Conclusion

In summary, we propose an  $\text{FeX}_2$ -semiconductor photocatalytic system for halogenation of hydrocarbons using earth abundant  $\text{NaBr}$  and  $\text{NaCl}$  as the halogen source under mild conditions. The presence of  $\text{FeX}_2$  boosts the photo-catalytic reduction of molecular oxygen and consumption of ROS, leading to a rapid generation of elemental halogen and halogen radicals from  $\text{NaBr}$  and  $\text{NaCl}$  for either direct halogenation and indirect halogenation via the formation of  $\text{FeX}_3$ . The coupling of  $\text{FeX}_2$  with a semiconductor photocatalyst enables continuous halogenation of a wide range of hydrocarbons with high efficiency, selectivity, and stability, which is critical for production at larger scale under flow conditions. Further work in realizing regioselective halogenation of complicated molecules will be crucial for synthetic applications, which may be realized by immobilizing efficient homogeneous catalysts on the heterogeneous system.

## Acknowledgements

R.S. thanks the NSFC (project number: 21972100), the Project of Innovation and Entrepreneurship of Jiangsu Province (grant numbers: JSSCRC202010539), and the Suzhou Foreign Academician Workstation (project number: SWY2022001) for financial support. E.R. thanks the financial support from EPSRC (EP/T013079/1). F.R. is grateful to the Canada Research Chairs program for partial salary support. We also acknowledge support from the Soochow Municipal Laboratory for Low Carbon Technologies and Industries.

## Conflict of Interest

The authors declare no conflict of interest.

## Data Availability Statement

The data that support the findings of this study are available in the Supporting Information of this article.

**Keywords:** Flow Synthesis · Green Chemistry · Halogenation · Heterogeneous Photocatalysis · Oxidant Free

[1] a) B. Gál, C. Bucher, N. Z. Burns, *Mar. Drugs* **2016**, *14*, 206; b) R. Lin, A. P. Amrute, J. Perez-Ramirez, *Chem. Rev.* **2017**, *117*, 4182–4247; c) I. Saikia, A. J. Borah, P. Phukan, *Chem.*

- Rev.* **2016**, *116*, 6837–7042; d) F. Zhang, *Acta Phys.-Chim. Sin.* **2008**, *24*, 1335–1341.
- [2] a) Y. Nishina, H. Hashimoto, N. Kimura, N. Miyata, T. Fujii, B. Ohtani, J. Takada, *RSC Adv.* **2012**, *2*, 6420–6423; b) H. Suzuki, Y. Nishina, *Bull. Chem. Soc. Jpn.* **2017**, *90*, 74–78; c) G. S. Tyndall, J. J. Orlando, T. J. Wallington, J. Sehested, O. J. Nielsen, *J. Phys. Chem.* **1996**, *100*, 660–668.
- [3] a) D. Cantillo, C. O. Kappe, *React. Chem. Eng.* **2017**, *2*, 7–19; b) P. S. Skell, H. N. Baxter, *J. Am. Chem. Soc.* **1985**, *107*, 2823–2824; c) M. Xiang, C. Zhou, X. L. Yang, B. Chen, C. H. Tung, L. Z. Wu, *J. Org. Chem.* **2020**, *85*, 9080–9087; d) H. Xin, S. Yang, B. An, Z. An, *RSC Adv.* **2017**, *7*, 13467–13472.
- [4] a) A. J. McMillan, M. Sieńkowska, P. Di Lorenzo, G. K. Gransbury, N. F. Chilton, M. Salamone, A. Ruffoni, M. Bietti, D. Leonori, *Angew. Chem. Int. Ed.* **2021**, *60*, 7132–7139; b) Y. Nishina, B. Ohtani, K. Kikushima, *Beilstein J. Org. Chem.* **2013**, *9*, 1663–1667; c) D. A. Rogers, R. G. Brown, Z. C. Brandenburg, E. Y. Ko, M. D. Hopkins, G. LeBlanc, A. A. Lamar, *ACS Omega* **2018**, *3*, 12868–12877; d) V. A. Schmidt, R. K. Quinn, A. T. Brusoe, E. J. Alexanian, *J. Am. Chem. Soc.* **2014**, *136*, 14389–14392.
- [5] a) A. Fawcett, M. J. Keller, Z. Herrera, J. F. Hartwig, *Angew. Chem. Int. Ed.* **2021**, *60*, 8276–8283; b) R. K. Quinn, Z. A. Konst, S. E. Michalak, Y. Schmidt, A. R. Szklarski, A. R. Flores, S. Nam, D. A. Horne, C. D. Vanderwal, E. J. Alexanian, *J. Am. Chem. Soc.* **2016**, *138*, 696–702.
- [6] a) I. Ghosh, J. Khamrai, A. Savateev, N. Shlapakov, M. Antonietti, B. König, *Science* **2019**, *365*, 360–366; b) N. S. Liebov, J. M. Goldberg, N. C. Boaz, N. Coutard, S. E. Kalman, T. Zhuang, J. T. Groves, T. B. Gunnoe, *ChemCatChem* **2019**, *11*, 5045–5054.
- [7] a) Y. Çimen, S. Akyüz, H. Türk, *New J. Chem.* **2015**, *39*, 3894–3899; b) W. Lu, M. Zhao, M. Li, *Synthesis* **2018**, *50*, 4933–4939; c) M. Zhao, W. Lu, *Org. Lett.* **2017**, *19*, 4560–4563; d) M. Zhao, W. Lu, *Org. Lett.* **2018**, *20*, 5264–5267.
- [8] a) T. Hering, B. Muhldorf, R. Wolf, B. König, *Angew. Chem. Int. Ed.* **2016**, *55*, 5342–5345; b) L. Zhang, X. Hu, *Chem. Sci.* **2017**, *8*, 7009–7013.
- [9] a) W. C. Baird, Jr., J. H. Surridge, *J. Org. Chem.* **1970**, *35*, 3436–3442; b) P. Lian, W. Long, J. Li, Y. Zheng, X. Wan, *Angew. Chem. Int. Ed.* **2020**, *59*, 23603–23608; c) W. Wu, Z. Fu, X. Wen, Y. Wang, S. Zou, Y. Meng, Y. Liu, S. R. Kirk, D. Yin, *Appl. Catal. A* **2014**, *469*, 483–489.
- [10] a) S. Liu, Q. Zhang, X. Tian, S. Fan, J. Huang, A. Whiting, *Green Chem.* **2018**, *20*, 4729–4737; b) G. B. Shul'pin, A. N. Druzhinina, *Mendeleev Commun.* **1992**, *2*, 36–37; c) W. Wu, X. He, Z. Fu, Y. Liu, Y. Wang, X. Gong, X. Deng, H. Wu, Y. Zou, N. Yu, D. Yin, *J. Catal.* **2012**, *286*, 6–12.
- [11] A. Maldotti, G. Varani, A. Molinari, *Photochem. Photobiol. Sci.* **2006**, *5*, 993–995.
- [12] a) D. Lv, Y. Li, W. Qiao, D. Zhang, Y. Mai, N. Cai, H. Xiang, Y. Li, H. Niemantsverdriet, W. Hao, R. Su, *Appl. Catal. B* **2022**, *309*, 121264; b) Y. Sun, Y. Li, Z. Li, D. Zhang, W. Qiao, Y. Li, H. Niemantsverdriet, W. Yin, R. Su, *ACS Catal.* **2021**, *11*, 15083–15088; c) K. Muralirajan, R. Kancherla, J. A. Bau, M. R. Taksande, M. Qureshi, K. Takanebe, M. Rueping, *ACS Catal.* **2021**, *11*, 14772–14780; d) A. Takabayashi, F. Kishimoto, H. Tsuchiya, H. Mikami, K. Takanebe, *Nanoscale Adv.* **2023**, *5*, 1124–1132; e) H. Zhang, Y. Dong, D. Li, G. Wang, Y. Leng, P. Zhang, H. Miao, X. Wu, P. Jiang, Y. Zhu, *FlatChem* **2021**, *26*, 100232.
- [13] a) J. Jia, J. Zhang, F. Wang, L. Han, J. Z. Zhou, B. W. Mao, D. Zhan, *Chem. Commun.* **2015**, *51*, 17700–17703; b) F. Parrino, G. Camera Roda, V. Loddo, L. Palmisano, *Angew. Chem. Int. Ed.* **2016**, *55*, 10391–10395; c) F. Parrino, G. Camera Roda, V. Loddo, L. Palmisano, *J. Catal.* **2018**, *366*, 167–175; d) T. Rath, A. Urich, A. Luken, G. Zhao, A. Rittermeier, M. Muhler, *ChemSusChem* **2019**, *12*, 2725–2731.
- [14] a) Y. Markushyna, C. M. Schusslbauer, T. Ullrich, D. M. Guldi, M. Antonietti, A. Savateev, *Angew. Chem. Int. Ed.* **2021**, *60*, 20543–20550; b) Y. Markushyna, C. Teutloff, B. Kurpil, D. Cruz, I. Laueremann, Y. Zhao, M. Antonietti, A. Savateev, *Appl. Catal. B* **2019**, *248*, 211–217.
- [15] Q. Zhang, S. Liu, X. Tian, Y. Liu, S. Fan, B. Huang, A. Whiting, *Green Chem.* **2022**, *24*, 384–393.
- [16] Z. Luo, Y. Meng, X. Gong, J. Wu, Y. Zhang, L. W. Ye, C. Zhu, *Chin. J. Chem.* **2020**, *38*, 173–177.
- [17] a) D. M. Bulman, S. P. Mezyk, C. K. Remucal, *Environ. Sci. Technol.* **2019**, *53*, 4450–4459; b) H. Selcuk, J. J. Sene, M. V. Zanon, H. Z. Sarikaya, M. A. Anderson, *Chemosphere* **2004**, *54*, 969–974.
- [18] I. Chorkendorff, J. W. Niemantsverdriet, *Concepts of Modern Catalysis and Kinetics*, Wiley, Hoboken, **2003**, pp. 401–442.
- [19] Q. Wu, J. Ye, W. Qiao, Y. Li, J. W. Niemantsverdriet, E. Richards, F. Pan, R. Su, *Appl. Catal. B* **2021**, *291*, 120118.
- [20] F. Han, D. Zhang, S. Salli, J. Ye, Y. Li, F. Rosei, X.-D. Wen, H. Niemantsverdriet, E. Richards, R. Su, *ACS Catal.* **2022**, *12*, 248–255.
- [21] K. Reszka, P. Bilski, R. H. Sik, C. F. Chignell, *Free Radical Res. Commun.* **1993**, *19 Suppl 1*, S33–44.
- [22] D. Zhang, P. Ren, W. Liu, Y. Li, S. Salli, F. Han, W. Qiao, Y. Liu, Y. Fan, Y. Cui, Y. Shen, E. Richards, X. Wen, M. H. Rummeli, Y. Li, F. Besenbacher, H. Niemantsverdriet, T. Lim, R. Su, *Angew. Chem. Int. Ed.* **2022**, *61*, e202204256.
- [23] a) R. Ameta, A. K. Chohadia, A. Jain, P. B. Punjabi in *Advanced Oxidation Processes for Waste Water Treatment* (Eds.: S. C. Ameta, R. Ameta), Academic Press, New York, **2018**, pp. 49–87; b) Q. Yi, J. Ji, B. Shen, C. Dong, J. Liu, J. Zhang, M. Xing, *Environ. Sci. Technol.* **2019**, *53*, 9725–9733.
- [24] Y. Li, P. Ren, D. Zhang, W. Qiao, D. Wang, X. Yang, X. Wen, M. H. Rummeli, H. Niemantsverdriet, J. P. Lewis, F. Besenbacher, H. Xiang, Y. Li, R. Su, *ACS Catal.* **2021**, *11*, 4338–4348.
- [25] Y. Li, Y. Li, C. Hu, X. Wen, H. Xiang, Y. Li, H. Niemantsverdriet, R. Su, *Green Chem.* **2022**, *24*, 7622–7629.



